

Electronic Structures of MgB₂ under Uniaxial and Hydrostatic Compression

Kazuaki KOBAYASHI* and Kazuo YAMAMOTO¹,

Advanced Materials Laboratory, National Institute for Materials Science, Namiki 1-1, Tsukuba-shi, Ibaraki 305-0044

¹*Kanagawa Institute of Technology, 1030 Shimo-ogino, Atsugi, Kanagawa 243-0292*

(Received October 24, 2018)

Electronic and lattice properties of MgB₂ under uniaxial and hydrostatic compression are calculated. Lattice properties are optimized automatically by using the first-principles molecular dynamics (FPMD) method. Features of the electronic band structures under uniaxial and hydrostatic compression are quite different each other.

KEYWORDS: MgB₂, uniaxial compression, high pressure, first-principles, electronic structure, phonon frequency

§1. Introduction

Very recently, a new high T_c intermetallic superconductor material MgB₂ ($T_c = 39$ K) was discovered by J. Akimitsu group.¹⁾ MgB₂ has a AlB₂ crystal symmetry (P6/mmm) and the number of atoms in a unit cell is three. Already, a variety of extended experimental^{2, 3, 4, 5, 6)} and theoretical^{7, 8, 9, 10, 11, 12, 13, 14)} studies have been devoted.¹⁵⁾ The electronic structures of MgB₂ under high pressure (hydrostatic)¹³⁾ and with different lattice constants¹⁴⁾ are calculated by FLAPW, respectively.

In this study, we calculate the electronic and lattice properties of MgB₂ under uniaxial compression by using the first-principles molecular dynamics (FPMD) and to compare with results under hydrostatic compression. It is possible to obtain the optimized lattice properties under high pressure conditions using FPMD. We investigate the changes of electronic band structures under a variety of compression (uniaxial, hydrostatic, varying the c/a ratio). Phonon frequencies at the Γ point under uniaxial and hydrostatic compression are calculated in this study.

§2. Method of Calculation

The present calculation is based on the local density approximation in the density functional theory^{16, 17)} with the Wigner interpolation formula¹⁸⁾ for the exchange-correlation. The optimized pseudopotential (Mg and B) by Troullier and Martins (TM)¹⁹⁾ is used in order to reduce the number of plane waves. Non-local parts of pseudopotential are transformed to the Kleinman-Bylander separable forms.²⁰⁾ No ghost bands by this treatment are found in our calculation. A partial core correction (PCC)²¹⁾ is considered for Mg pseudopotential. The wave function is expanded in plane waves, and the energy cutoff is 81 Ry with the maximum number of plane waves

being about 2000. The number of sampling k-points is 95 in the 1/24 of the Brillouin zone (BZ) for all calculated systems. In the cell optimization, the number of k-points is fixed because a change of the c/a ratio under compression is not so large ($c/a = 0.868 \sim 1.123$).

The outline of our calculational process with the cell optimization is as follows. In this calculation, the system has kept to the AlB₂ crystal symmetry in the process of the cell optimization. Therefore, it does not discuss a structural phase transformation under uniaxial and hydrostatic compression in this study. At first, an electronic part is quenched to the ground state of a given initial lattice parameter, and optimization of electronic and unit cell shape parts is carried out simultaneously in the next step. Stresses²²⁾ acting on unit cell surfaces are calculated, and the lattice parameters are tuned by using them. We can estimate that a numerical error of the calculated pressure is less than about 1 GPa. There is no effect to discuss qualitatively although this value (1 GPa) may be slightly large.

We calculate in three conditions as follows. The first is the uniaxial compression. The uniaxial compression acts along a direction of c -axis. Values of external compression along a - and b -axis are 0 GPa in this case. The second is the hydrostatic compression. The third is to vary the c/a ratio when the values of a and b are fixed in the equilibrium lattice parameters. In the case of varying the c/a ratio, all surfaces of the unit cell have non-zero internal pressures.

§3. Results and Discussion

The optimized lattice properties in this calculation are tabulated in Table I.

Calculated bulk modulus of MgB₂ is 145 GPa, which agrees with other theoretical result.¹³⁾ A heat of formation of MgB₂ is 0.61 eV/cell. The calculated equilibrium lattice constant of c -axis is shorter by 3 % than that of experiment.¹⁾ The number of sampling k-points (= 95) may be insufficient for discussing quantitatively the

* Present author's (K. K.) URL address:
<http://www.geocities.co.jp/Technopolis/4765/index.html>

Table I. Equilibrium lattice constants[Å] and the c/a ratio of MgB₂. “Pz” indicates the uniaxial compression along c -axis. “P” indicates the hydrostatic compression. “ c/a ” indicates the varying c/a . The value of compression “ c/a ” indicates that along c -axis.

	c	a	c/a
0 GPa	3.421	3.047	1.123
10 GPa(Pz)	3.307	3.053	1.083
20 GPa(Pz)	3.183	3.067	1.038
30 GPa(Pz)	3.045	3.091	0.985
40 GPa(Pz)	2.932	3.109	0.943
50 GPa(Pz)	2.838	3.125	0.908
10 GPa(P)	3.324	2.998	1.109
20 GPa(P)	3.246	2.958	1.097
30 GPa(P)	3.179	2.923	1.088
40 GPa(P)	3.122	2.894	1.079
50 GPa(P)	3.072	2.868	1.071
22.3 GPa(c/a)	3.175	3.047	1.042
48.4 GPa(c/a)	2.910	3.047	0.955
84.6 GPa(c/a)	2.646	3.047	0.868
Exp ¹⁾	3.524	3.086	1.142

electronic and lattice properties because MgB₂ is metallic. In addition, this number is not adjusted in varying the unit cell volume. There is no problem for discussing qualitatively the electronic band structure changes under uniaxial and hydrostatic compression in this study. To check the convergence, we also calculate in the condition of the 259 k-points and 100 Ry under 0 GPa. A deviation of the equilibrium lattice constants is less than about 0.01 Å, and slightly improve the error of the lattice constant of c -axis from 3 % to 2.6 %.

The electronic band structures of the optimized lattice parameters are calculated. The electronic band structures under uniaxial compression (0, 20, 50 GPa) are shown in Fig. 1. The electronic band structures under hydrostatic compression (20, 50 GPa) are also shown in Fig. 1. The electronic band structure ($c/a = 0.955$, Pz = 48.4 GPa) in varying the c/a ratio is also shown in Fig. 1. As a result, the electronic band structures at 20, 50 GPa under hydrostatic compression are similar to that at 0 GPa. The small change of the c/a ratio under hydrostatic compression indicates the isotropic compressibility. This trend agrees with the other theoretical study¹³⁾ although the c/a ratio (= 1.123, P = 0 GPa) at present study is slightly different from the other theoretical result (= 1.1468).¹³⁾ The widths of band at 20, 50 GPa is larger than that at 0 GPa (that of 50 GPa is largest) as shown in Table II. On the other hand, the electronic structures under uniaxial compression are quite different from those under hydrostatic compression at the Fermi level. The σ bands at the Γ -A line shift to lower energy as the pressure increase. The electronic structure with varying the c/a ratio ($c/a = 0.955$, Pz = 48.4 GPa) is also different from those under hydrostatic

compression as shown in Fig. 1. This band structure ($a = a_0$ and $c = 0.85c_0$, a_0 and c_0 are the calculated equilibrium lattice constant in this study.) is corresponding to that of $a = a_0$ and $c = 0.8c_0$ ¹⁴⁾ (a_0 and c_0 ²³⁾) and they are similar to each other.

We calculate density of states (DOS) at 0 GPa, 50 GPa(hydrostatic), 50 GPa(uniaxial), nearly 50 GPa(varying c/a , Pz = 48.4 GPa). The density of states at Fermi level ($N(\epsilon_f)$) at 0 GPa, 50 GPa(hydrostatic), 50 GPa(uniaxial), nearly 50 GPa(varying c/a) are 1.0, 0.94, 0.71, 0.77, respectively, where the values of $N(\epsilon_f)$ are normalized as 1.0 for $N(\epsilon_f)$ at 0 GPa. The number of k-points is not enough to discuss quantitatively the values of $N(\epsilon_f)$. The values of $N(\epsilon_f)$ under compression are smaller than that under 0 GPa and the decrease of $N(\epsilon_f)$ under anisotropic compression is larger than that under hydrostatic (isotropic) compression. The density of states at 0 GPa and 50 GPa(hydrostatic) are similar to each other except for the band width. The density of states at 50 GPa (uniaxial) and nearly 50 GPa(varying c/a) are quite different from those at 0 GPa and 50 GPa(hydrostatic).

Table II. The values of the band width from the bottom of the valence band to the Fermi level. “Pz” indicates the uniaxial compression along c -axis. “P” indicates the hydrostatic compression. “ c/a ” indicates the varying c/a .

	Width(eV)	c/a
0 GPa	12.6	1.123
20 GPa(Pz)	12.9	1.038
50 GPa(Pz)	14.0	0.908
20 GPa(P)	13.3	1.097
50 GPa(P)	14.0	1.071
48.4 GPa(c/a)	13.9	0.955

We calculate phonon frequencies f_w at the Γ point under 0 GPa, 50 GPa(uniaxial) and 50 GPa(hydrostatic) compression as shown in Table III. The calculated displacements of atoms in the unit cell are shown in Fig. 4. The number of k-points is 512 ($8 \times 8 \times 8$) in the whole Brillouin zone (BZ) in order to obtain the accurate phonon frequencies because this calculation does not consider symmetry due to the displacement of atoms in the unit cell. The values of the phonon frequencies at the Γ point are in good agreement with other theoretical results^{7,9,12)} except for the E_{2g} mode. The discrepancies of the phonon frequencies at the E_{1u} , A_{2u} , B_{1g} modes at present and the other theoretical studies^{7,9,12)} are very small. On the other hand, the values of the E_{2g} mode (629[Present], 470,⁷⁾ 585,¹²⁾ 665⁹⁾ cm⁻¹) in the theoretical calculations has a large difference. The values of phonon frequencies under compression are larger than that under 0 GPa because the cell volume is shrunk by compression. Values of the volume ratio (V/V_0 , V_0 :equilibrium volume) are 0.795 ($P = 50$ GPa) and 0.872 ($Pz = 50$ GPa), respectively. The deviations of lattice changes are -5.9 % ($P = 50$ GPa), +2.6 % ($Pz =$

50 GPa) along a -axis and -17.0 % ($P = 50$ GPa), -10.2 % ($P_z = 50$ GPa). The value of the phonon frequency at the E_{2g} mode under hydrostatic compression (50 GPa) is 886 cm^{-1} , in which the increase of the phonon frequency is largest in all calculated phonon frequencies. In particular, the change of the phonon frequency at the E_{2g} mode under uniaxial compression ($P_z = 50$ GPa) is largest in the four modes in spite of the elongation of a B-B distance on the B layer. The σ bands at the $\Gamma - A$ line are completely occupied by uniaxial compression. This occupation means that the number of electrons with regard to σ bonding in the B layer increases. Increasing σ bonding electrons under uniaxial compression is to strengthen the B-B bond, which leads to increase the value of the phonon frequency at E_{2g} mode. On the other hand, the lattice change (-5.9 %) under hydrostatic compression ($P = 50$ GPa) directly strengthens the B-B bonding although the σ bands at the $\Gamma - A$ line are unoccupied.

Table III. The values of the phonon frequencies f_w (cm^{-1}) at the Γ point. “ P_z ” indicates the uniaxial compression along c -axis. “ P ” indicates the hydrostatic compression.

	f_w (0 GPa)	f_w ($P = 50$ GPa)	f_w ($P_z = 50$ GPa)
E_{1u}	348	500	513
A_{2u}	398	594	517
E_{2g}	629	886	851
B_{1g}	707	814	747

§4. Summary

We calculate the electronic and lattice properties of MgB₂ under uniaxial, hydrostatic compression and varying the c/a ratio by using FPMD. The phonon frequencies at the Γ point under 0 GPa, 50 GPa (uniaxial) and 50 GPa (hydrostatic) are calculated. It is possible to explain the increasing the phonon frequencies under compression by the analysis of the electronic band structures. Although the width of the electronic band structure is spread by compression, the band structure change is not so large under hydrostatic compression. The electronic band structure changes (σ bands) are quite large under uniaxial compression and varying the c/a ratio at the Fermi level. We think that it is very important to investigate the difference of the electronic band structures (σ bands) at the Fermi level under hydrostatic, uniaxial and varying the c/a ratio.

More accurate study (the number of k-points, possibility of a pressure induced phase transition, etc.) is a near future task.

Acknowledgements

We would like to thank Dr. M. Arai, Dr. K. Takemura, Dr. S. Higai and Prof. S. Suzuki for valuable discussions. The numerical calculations were performed at The National Institute for Research in Inorganic materi-

als (AlphaServer GS140 for COMPAQ). The author also thanks the staff of The Supercomputer Center (System A, B), Institute for Solid State Physics (ISSP), University of Tokyo for the facilities provided by them.

-
- [1] J. Nagamatsu, N. Nakagawa, T. Muranaka, Y. Zenitani and J. Akimitsu: Nature **410** (2001) 63.
 - [2] S. L. Bud'ko, G. Lapertot, C. Petrovic, C. E. Cunningham, N. Anderson and P. C. Canfield: Phys. Rev. Lett., **86** (2001)1877.
 - [3] Y. Takano, H. Takeya, H. Fujii, H. Kumakura, T. Hatano, K. Togano, H. Kito and H. Ihara: cond-mat/0102167.
 - [4] B. Lorenz, R. L. Meng and C. W. Chu: cond-mat/0102264.
 - [5] E. Saito, T. Taknenobu, T. Ito, Y. Iwasa, K. Prassides: cond-mat/0102511
 - [6] T. Tomita, J. J. Hamlin, J. S. Schilling, D. G. Hinks and J. D. Jorgensen: cond-mat/0103538.
 - [7] J. Kortus, I. I. Mazin, K. D. Belashchenko, V. P. Antropov and L. L. Boyer: Phys. Rev. Lett., Vol. 86, May 7 (2001).
 - [8] K. D. Belaschenko, M. van Schilfgaarde and V. P. Antropov: cond-mat/0102290.
 - [9] G. Satta, G. Profeta, F. Bernardini, A. Continenza and S. Massidda: cond-mat/0102358.
 - [10] J. M. An, W. E. Pickett: Phys. Rev. Lett., Vol. 86, May 7 (2001).
 - [11] S. Suzuki, S. Higai, K. Nakao: J. Phys. Soc. Jpn. **70**, No. 5 (2001).
 - [12] Y. Kong, O.V. Dolgov, O. Jepsen and O.K. Andersen: cond-mat/0102499.
 - [13] I. Loa and K. K. Syassen: accepted by Solid State Commun.
 - [14] X. Wan, J. Dong, H. Weng and D. Y. Xing: cond-mat/0104216.
 - [15] As for other studies, see in the web site of “High T_c Update” (URL: <http://www.iitap.iastate.edu/htcu/htcu.html>).
 - [16] P. Hohenberg and W. Kohn: Phys. Rev. **136** (1964) B864.
 - [17] W. Kohn and L. J. Sham: Phys. Rev. **140** (1965)A1133.
 - [18] E. Wigner: Phys. Rev. **46** (1934)1002.
 - [19] N. Troullier and J. L. Martins: Phys. Rev. B, **43** (1991)1993.
 - [20] L. Kleinman and D. M. Bylander: Phys. Rev. Lett., **48** (1982)1425.
 - [21] S. G. Louie, S. Froyen and M. L. Cohen, Phys. Rev. **B26** (1982)1738.
 - [22] O. H. Nielsen and R. M. Martin: Phys. Rev. **B32** (1985)3792.
 - [23] M. E. Jones and R. E. Marsh: J. Am. Chem. Soc. **76**(1954)1434.

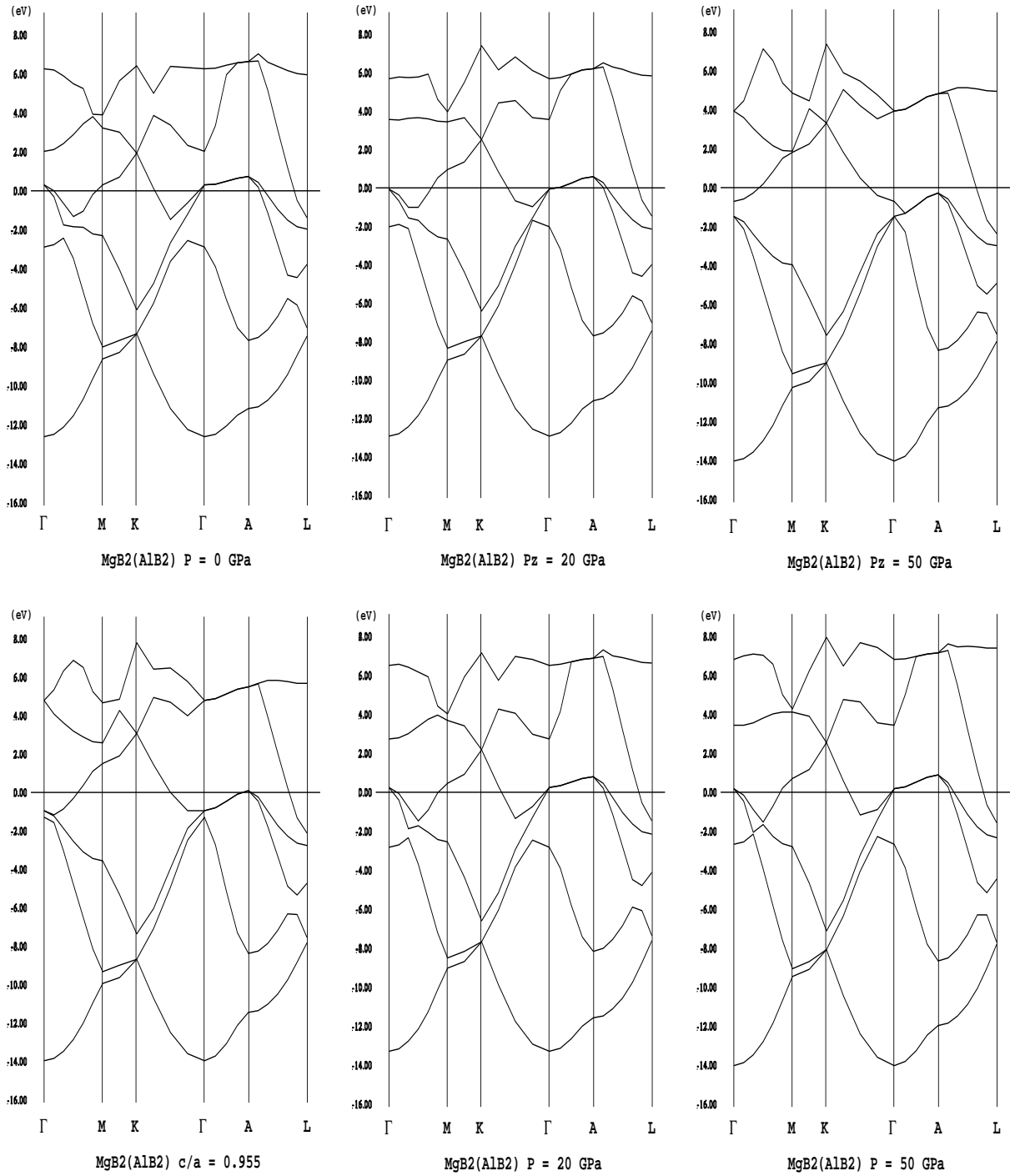


Fig. 1. Energy band structures of MgB₂ under uniaxial and hydrostatic compression, $c/a = 0.955$ (varying the c/a ratio). The Fermi level is indicated by the horizontal line.

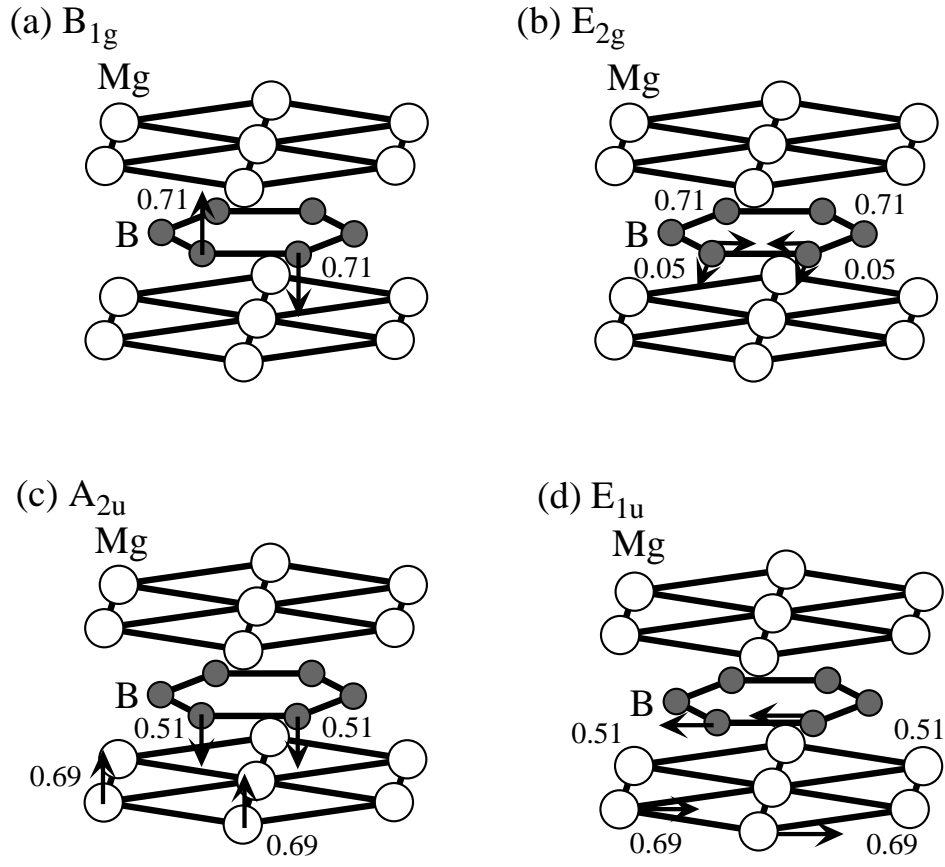


Fig. 2. Atomic displacements in the unit cell for phonon frequencies at E_{1u}, A_{2u}, E_{2g}, B_{1g} modes. The arrows indicate the directions of atomic displacements in the unit cell.